CZECH TECHNICAL UNIVERSITY IN PRAGUE

FACULTY OF NUCLEAR SCIENCES AND PHYSICAL ENGINEERING

Department of Physics

Theoretical description of nuclei with non-zero strangeness

RESEARCH PROJECT

Autor: **Bc. Martin Schäfer**

Supervisor: **RNDr. Jiří Mareš, CSc.**

Academic year: **2013/2014**

Acknowledgement

I would like to thank my supervisor Dr. Jiří Mareš for his invaluable advice and professional support and Dr. Axel-Pérez Obiol for useful discussions during this work. I would also like to thank Dr. Thomas Neff and prof. Hans Feldmeier for introducing me into the Fermion Molecular Dynamics model.

Contents

Chapter 1

Introduction

Increasingly sophisticated knowledge of the nucleon-nucleon interaction in recent years gave us an opportunity, with the help of many-body models and more precise numerical approaches, to calculate the energy of ground and excited states of nuclei with very small deviations from experimental values. Moreover, these calculations provide us with information about the nuclear structure which corresponds to relevant quantum numbers. From the existence of α-decay we can deduce that alpha clusters should exist in a nucleus even before the decay itself. Using the knowledge of the NN interaction we should be able to calculate the multiparticle wave function relevant to the ground or excited states of a given nucleus for corresponding quantum numbers.The formation of nuclear clusters inside a nucleus is an explicit consequence of a given NN interaction. This issue has been widely studied by Thomas Neff and Hans Feldmeier at GSI [1], [2] and [3]. The basic framework of their calculations is the Fermion Molecular Dynamics model (FMD) [4]. This model in its early stages was used to describe the fragmentation during nuclear reactions [5]. Later it has been applied in nuclear structure calculations.

The FMD model proved itself appropriate for incorporating the Unitary Correlation Method (UCOM), as described in the PhD. thesis of Thomas Neff [6]. This method allows us to perform calculations with realistic NN potentials. The basic concept of UCOM is to define a unitary correlation operator which describes the short range forces between nucleons (the unitary operator reflects tensor and radial part of the correlations between nucleons). The unitary operators could act on state vectors or on two-body potential in its operator form. We could say that the UCOM also improves the FMD model since the applied Hartree-Fock method for the basis of trial Gaussian wave functions with spin and isospin parts is not able to describe short range correlations properly.

The aim of the research project is to develop from the very beginning the computational code within the Fermion Molecular Dynamics framework which could be

further extended and applied in calculations of the structure of hypernuclei. Thus the program should be flexible enough to allow to incorporate, without substantial modifications, also baryons with non-zero strangeness, i.e. Λ, Σ^0, Σ^+, Σ^-.

In this work we primarily consider only protons and neutrons since we would like to check the correctness of our model and compare our results with existing FMD calculations of ordinary nuclei [4]. In the next step, strange baryons and corresponding baryon-baryon interactions will be added to the previously tested FMD program for nuclear part in order to perform calculations of hypernuclei.

In order to test our model we use the effective VolkovV2 interaction with Majorana exchange parameter M0.0 [7]. The ground state and binding energy of ^{3}H and ^{4}He are successfully determined and compared with the other FMD model calculations [4]. To evaluate the computational complexity of the program we applied the VolkovV2 potential also for the calculations of ^{5}He and ^{6}He. Since the VolkovV2 interaction with M0.0 does not describe these nuclei properly we discuss only the duration of the minimization process as a function of the nuclear mass number.

This work consists of 6 chapters and 4 appendices. In the second chapter, the FMD model is presented and the calculation of the expectation value of the Hamiltonian with the parity, angular momentum and center of mass projected many-body wave function is discussed. The used effective VolkovV2 interaction is introduced in the third chapter and the structure of the FMD program is discussed in Chapter 4. The results of the FMD calculations of the ^{3}H and ^{4}He ground states and the computational complexity of the FMD program are presented in the fifth chapter. Conclusions are summarized in Chapter 6. The antisymmetrization of the many-body wave function, derivation of the expectation value formulae, auxiliary matrices and the calculations of derivatives are given in Appendix A, B, C, and D.

This work was continuously consulted with H. Feldmeier and T. Neff from GSI.

Chapter 2

Fermion Molecular Dynamics

The Fermion Molecular Dynamics model describes a system consisting of fermions. Therefore, the many-body states have to be antisymmetrized. To satisfy this condition we approximate the many-body wave function by Slater determinant.

Single particle basis states are described as Gaussian wave packets-this provides the FMD model with very flexible basis. Consequently, the Gaussian wave packets provide appreciable flexibility during the variation process of the expectation value of a Hamiltonian. They are also suitable to describe the cluster structure of nuclei as well as the structure of neutron-rich "halo" nuclei.

The description of nuclear or hypernuclear constituents using the Gaussian wave packets allows to study localization of single particles in a nucleus. The FMD model can be compared with widely used Antisymmetrized Molecular Dynamics (AMD) model [8]. The main difference is that the AMD model works with the Gaussian wave packets with the same width parameter for each single particle state. This simplification allows to use less complicated imaginary time evolution [9] to minimize the expectation value of the Hamiltonian at the cost of less flexible basis.

Other, less significant difficulty, is the non-orthogonality of single particle basis. This can be fully resolved during the analytical evaluation of expectation values.

2.1 Single particle state

To define the basic framework of FMD we begin with the definition of a single particle state $|q\rangle$ described by a spatial, spin and isospin part

$$|q\rangle = \left|a, \vec{b}\right\rangle \otimes \left|\chi^{\uparrow}, \chi^{\downarrow}\right\rangle \otimes |t\rangle \,. \tag{2.1}$$

The isospin part $|t\rangle$ does not change during calculations and remains constant. According to assumptions of the FMD model the spatial part is represented by the

Gaussian wave packet which is in x-representation expressed as

$$\left\langle \vec{x} \right| \left. a, \vec{b} \right\rangle = e^{-\frac{(\vec{x}-\vec{b})^2}{2a}}. \tag{2.2}$$

There are four complex parameters involved : the complex width $a = \mathrm{Re}a + \mathrm{iIm}a$ and the complex "position-like" parameter described by the vector $\vec{b} = \mathrm{Re}\vec{b} + \mathrm{iIm}\vec{b}$.

The spin part is represented by two complex parameters : the spin up ($\chi^{\uparrow}$) and the spin down ($\chi^{\downarrow}$) :

$$\left|\chi^{\uparrow}, \chi^{\downarrow}\right\rangle = \begin{pmatrix} \chi^{\uparrow} \\ \chi^{\downarrow} \end{pmatrix}. \tag{2.3}$$

Overall we have twelve independent parameters which fully describe the single particle state.

$$\begin{aligned} a &= \mathrm{Re}a + \mathrm{iIm}a, \\ b_1 &= \mathrm{Re}b_1 + \mathrm{iIm}b_1, \\ b_2 &= \mathrm{Re}b_2 + \mathrm{iIm}b_2, \\ b_3 &= \mathrm{Re}b_3 + \mathrm{iIm}b_3, \\ \chi^{\uparrow} &= \mathrm{Re}\chi^{\uparrow} + \mathrm{iIm}\chi^{\uparrow}, \\ \chi^{\downarrow} &= \mathrm{Re}\chi^{\downarrow} + \mathrm{iIm}\chi^{\downarrow}. \end{aligned} \tag{2.4}$$

The scalar product of a state $|q\rangle$ given in (2.1) could be written as

$$\langle q| \, q\rangle = \left\langle a, \vec{b} \right| \left. a, \vec{b} \right\rangle \left\langle \chi^{\uparrow}, \chi^{\downarrow} \right| \left. \chi^{\uparrow}, \chi^{\downarrow} \right\rangle \langle t| \, t\rangle = \left(2\pi \frac{a^* a}{a^* + a} \right)^{3/2} e^{-\frac{(\vec{b}-\vec{b^*})^2}{2(a+a^*)}} (|\chi^{\uparrow}|^2 + |\chi^{\downarrow}|^2). \tag{2.5}$$

The mean position $\vec{x}$ and mean momentum $\vec{p}$ of a single particle state could be easily calculated giving physical meaning to the individual parameters describing spatial part

$$\vec{x} = \frac{\left\langle a, \vec{b} \right| \hat{\vec{x}} \left| a, \vec{b} \right\rangle}{\left\langle a, \vec{b} \right| \left. a, \vec{b} \right\rangle} = \frac{a^* \vec{b} + a\vec{b^*}}{a + a^*} = \frac{\mathrm{Re}a\mathrm{Re}\vec{b} + \mathrm{Im}a\mathrm{Im}\vec{b}}{\mathrm{Re}a}, \tag{2.6}$$

$$\vec{p} = \frac{\left\langle a, \vec{b} \right| \hat{\vec{p}} \left| a, \vec{b} \right\rangle}{\left\langle a, \vec{b} \right| \left. a, \vec{b} \right\rangle} = \mathrm{i}\frac{\vec{b^*} - \vec{b}}{a + a^*} = \frac{\mathrm{Im}\vec{b}}{\mathrm{Re}a}. \tag{2.7}$$

From (2.6) and (2.7) we can straightforwardly deduce that in the case of a particle with the mean momentum $\vec{p}$ equal to zero the mean position $\vec{x}$ is equal to real part of $\vec{b}$.

Furthermore, we must mention an important properties of single particle state

with respect to translation, parity and rotation operations. The action of the translation operator $\hat{U}(\vec{d})$ on a single particle state can be expressed as

$$\hat{U}(\vec{d})\left|a,\vec{b}\right\rangle \otimes \left|\chi^{\uparrow},\chi^{\downarrow}\right\rangle \otimes |t\rangle = \left|a,\vec{b}+\vec{d}\right\rangle \otimes \left|\chi^{\uparrow},\chi^{\downarrow}\right\rangle \otimes |t\rangle\,. \tag{2.8}$$

In the case of rotation represented by the operator $\hat{R}(\Omega)$ we must take into account that it acts both in the coordinate and spin space $\hat{R}(\Omega) = \hat{R}_{pos.}(\Omega)\otimes\hat{R}_{spin}(\Omega)$ and thus

$$\begin{aligned}\hat{R}(\Omega)\left\{\left|a,\vec{b}\right\rangle \otimes \left|\chi^{\uparrow},\chi^{\downarrow}\right\rangle \otimes |t\rangle\right\} &= \hat{R}_{pos.}(\Omega)\left|a,\vec{b}\right\rangle \otimes \hat{R}_{spin}(\Omega)\left|\chi^{\uparrow},\chi^{\downarrow}\right\rangle \otimes |t\rangle = \\ &= \left|a,\hat{R}_{pos.}(\Omega)\cdot\vec{b}\right\rangle \otimes \hat{R}_{spin}(\Omega)\left|\chi^{\uparrow},\chi^{\downarrow}\right\rangle \otimes |t\rangle\,.\end{aligned} \tag{2.9}$$

The effect of parity operation represented by operator $\hat{\Pi}$ can be written as

$$\hat{\Pi}\left|a,\vec{b}\right\rangle \otimes \left|\chi^{\uparrow},\chi^{\downarrow}\right\rangle \otimes |t\rangle = \left|a,-\vec{b}\right\rangle \otimes \left|\chi^{\uparrow},\chi^{\downarrow}\right\rangle \otimes |t\rangle\,. \tag{2.10}$$

2.2 Many-body state

The many-body state $|Q\rangle$ describing N particles occupies the Hilbert space $\mathscr{H}_N$. The many-body Hilbert space could be written as a tensor product of N single particle spaces $\mathscr{H}_1$ including position, spin and isospin part

$$\mathscr{H}_N = \mathscr{H}_1 \otimes \ldots \otimes \mathscr{H}_1. \tag{2.11}$$

Thus we can write the many-body state $|Q\rangle \in \mathscr{H}_N$ as

$$|Q\rangle = |q_1,\ldots,q_N\rangle = |q_1\rangle \otimes \ldots \otimes |q_N\rangle\,, \tag{2.12}$$

where $|q_i\rangle\,,\ i \in N$ represent the single particle states.

Denoting $|x_1,\ldots,x_N\rangle$ as both the position and quantum numbers of given single particle states we can write the many-body function $|Q\rangle$ in the Hartree approximation as a product of single particle states

$$\langle x_1,\ldots,x_N|\,Q\rangle = \langle x_1,\ldots,x_N|\,q_1,\ldots,q_N\rangle = \langle x_1|\,q_1\rangle\,\langle x_2|\,q_2\rangle\ldots\langle x_{N-1}|\,q_{N-1}\rangle\,\langle x_N|\,q_N\rangle\,. \tag{2.13}$$

Since the nuclear many-body wave function consists of N indistinguishable nucleons with spin one-half we require the many-body wave function to be fully antisymmetrized with respect to the exchange among nucleons. This is ensured by

applying the antisymmetrization operator $\hat{A}$ on the many-body wave function $|Q\rangle$

$$|Q_A\rangle = \hat{A}\,|Q\rangle = \frac{1}{N!}\sum_{P_i} sgn(P_i)\left|q_{P_i(1)}\right\rangle \otimes \ldots \otimes \left|q_{P_i(N)}\right\rangle . \tag{2.14}$$

The details of the antisymmetrization are presented in Appendix A.

The scalar product of antisymmetrized many-body wave function can be then written within the Hartree-Fock approximation as

$$\begin{aligned}\langle Q_A|\, Q_A\rangle = \langle Q|\, Q_A\rangle = \{\langle q_1| \otimes \ldots \otimes \langle q_N|\}\{\frac{1}{N!}\sum_{P_i} sgn(P_i)\left|q_{P_i(1)}\right\rangle \otimes \ldots \otimes \left|q_{P_i(N)}\right\rangle\} = \\ = \frac{1}{N!}\sum_{P_i} sgn(P_i)\left\langle q_1\right|\, q_{P_i(1)}\rangle \otimes \ldots \otimes \left\langle q_N\right|\, q_{P_i(N)}\rangle = \det|\mathrm{n}|,\end{aligned} \tag{2.15}$$

where we take into account that $\hat{A}$ is a projection operator and n stands for the single particle overlap matrix

$$\mathrm{n} = \begin{pmatrix} \langle q_1|\, q_1\rangle & \langle q_1|\, q_2\rangle & \cdots & \langle q_1|\, q_{N-1}\rangle & \langle q_1|\, q_N\rangle \\ \langle q_2|\, q_1\rangle & \langle q_2|\, q_2\rangle & \cdots & \langle q_2|\, q_{N-1}\rangle & \langle q_2|\, q_N\rangle \\ \vdots & \vdots & \ddots & \vdots & \vdots \\ \langle q_{N-1}|\, q_1\rangle & \langle q_{N-1}|\, q_2\rangle & \cdots & \langle q_{N-1}|\, q_{N-1}\rangle & \langle q_{N-1}|\, q_N\rangle \\ \langle q_N|\, q_1\rangle & \langle q_N|\, q_2\rangle & \cdots & \langle q_N|\, q_{N-1}\rangle & \langle q_N|\, q_N\rangle \end{pmatrix} \tag{2.16}$$

which consists of elements given in Eq. (2.5).

2.3 Expectation values

When calculating the expectation values of one and two-body operators we must emphasize from the beginning the non-orthogonality of the FMD basis. For the expectation value of a one-body operator $\hat{O}^{[1]}$ it holds

$$O^{[1]} = \frac{\langle Q|\, \hat{O}^{[1]}\, |Q_A\rangle}{\langle Q|\, Q_A\rangle} = \sum_{kl} \langle q_k|\, \hat{O}^{[1]}\, |q_l\rangle\, o_{lk}. \tag{2.17}$$

The expectation value of a two-body operator $\hat{O}^{[2]}$ can be expressed as

$$O^{[2]} = \frac{\langle Q|\, \hat{O}^{[2]}\, |Q_A\rangle}{\langle Q|\, Q_A\rangle} = \frac{1}{2}\sum_{klmn} \langle q_k, q_l|\, \hat{O}^{[2]}\, |q_m, q_n\rangle\, (o_{mk}o_{nl} - o_{nk}o_{ml}). \tag{2.18}$$

The overall properties of the multiparticle system in the FMD model are determined by the total Hamiltonian $\hat{H}$ which can be decomposed in the case of one and two-body operators as follows

$$\hat{H} = \hat{H}^{[1]} + \hat{H}^{[2]}, \tag{2.19}$$

where $\hat{H}^{[1]}$ denotes the one-body and $\hat{H}^{[2]}$ the two-body part of the Hamiltonian. In general, the total Hamiltonian can be written as the sum

$$\hat{H} = \sum_i \hat{H}_i^{[1]} + \sum_j \hat{H}_j^{[2]}, \tag{2.20}$$

where $\hat{H}_i^{[1]}$ and $\hat{H}_j^{[2]}$ are individual contributions to $\hat{H}$.

To calculate the expectation value E of the $\hat{H}$ we use the Eqs. (2.17), (2.18) and notation in (C.1). We get the following expression

$$\begin{aligned} E = \frac{\langle Q_A|\, \hat{H}\, |Q_A\rangle}{\langle Q_A|\, Q_A\rangle} &= \sum_i \frac{\langle Q_A|\, \hat{H}_i^{[1]}\, |Q_A\rangle}{\langle Q_A|\, Q_A\rangle} + \sum_j \frac{\langle Q_A|\, \hat{H}_j^{[2]}\, |Q_A\rangle}{\langle Q_A|\, Q_A\rangle} = \\ &= \sum_i \sum_{kl} \langle q_k|\, \hat{H}_i^{[1]}\, |q_l\rangle\, o_{lk} + \\ &+ \sum_j \frac{1}{2} \sum_{klmn} \langle q_k, q_l|\, \hat{H}_j^{[2]}\, |q_m, q_n\rangle\, (o_{mk}o_{nl} - o_{nk}o_{ml}) = \\ &= \sum_i \sum_{kl} H_{i\ kl}^{[1]}\, o_{lk} + \sum_j \frac{1}{2} \sum_{klmn} H_{j\ klmn}^{[2]} (o_{mk}o_{nl} - o_{nk}o_{ml}). \end{aligned} \tag{2.21}$$

In order to evaluate the expectation value E, the one-body $H_{i\ kl}^{[1]}$ and the two-body $H_{i\ klmn}^{[2]}$ matrix elements of each one-body and two-body operator in the total Hamiltonian have to be calculated.

2.4 Ground state

The intrinsic many-body wave function describing the ground state of a given nucleus is determined by minimizing the expectation value E of the operator $\hat{H} - \hat{T}_{cm}$ with respect to all parameters present in the antisymmetrized many-body state $|Q_A\rangle$. Here, $\hat{T}_{cm}$ denotes the center of mass kinetic energy. We search for the minimum of

E in the subspace of $q_i,\ i \in n$ parameters where N stands for the number of particle in a nucleus and q_i represents the set of parameters for i-th particle state (2.4)

$$E_{min} = \min_{q_1,\ldots,q_n} \frac{\langle Q|\, \hat{H} - \hat{T}_{cm}\, |Q_A\rangle}{\langle Q|\, Q_A\rangle}. \tag{2.22}$$

The number of parameter forming the subspace in which we are searching for the minimum increases considerably with the number of particles. Generally the large number of parameters makes the minimization process very specific. We applied the quasi-Newton method Software for Large-scale Bound-constrained Optimization L-BFGS-B [10], [4].

In each iteration of the above iteration step, we have to evaluate the gradient of E with respect to all parameters $q_i,\ i \in n$. Since the numerical calculation of relevant derivatives is computation demanding and the approximate calculation can cause slow convergence of the minimization routine or "false" convergence to local minima, we evaluate all derivatives analytically. The analytical calculation is specified in Appendix D, especially in Eqs. (D.4) and (D.5).

2.5 Projections

The subtraction of the center of mass kinetic energy in (2.22) is only approximate; to be more precise we should project the many-body function on the center of mass momentum equal zero. Furthermore, the ground state obtained from the minimization of the expectation value E_{min} (2.22) is an intrinsic state and generally it is a mixture of states with different quantum numbers. These difficulties are handled by using the center of mass, parity and angular momentum projection. In the following paragraphs we use the notation given in [1].

2.5.1 Center of mass projection

In order to project the many-body function $|Q\rangle$ with the momentum $\vec{P}_Q$ on a certain value of the total momentum $\vec{P}$ we use the projection operator $\hat{P}^{\vec{P}}$

$$\begin{aligned} \hat{P}^{\vec{P}}\,|Q\rangle &= \left|\vec{P}\right\rangle \left\langle \vec{P}\right|\, Q\Big\rangle = \delta(\vec{P}_Q - \vec{P}) \left|\vec{P}\right\rangle = \delta(\hat{\vec{P}} - \vec{P})\,|Q\rangle = \\ &= \frac{1}{(2\pi)^3} \int d^3x\, \exp\left\{-\mathrm{i}(\hat{\vec{P}} - \vec{P}) \cdot \vec{x}\right\} |Q\rangle\,, \end{aligned} \tag{2.23}$$

where we used the integral representation of the δ-function $\delta(\vec{P}_Q - \vec{P})$. Thus the projection operator $\hat{P}^{\vec{P}}$ can be written in the following form

$$\hat{P}^{\vec{P}} = \frac{1}{(2\pi)^3} \int d^3x \, \exp\left\{-\mathrm{i}(\hat{\vec{P}} - \vec{P}) \cdot \vec{x}\right\}. \tag{2.24}$$

The projection of $|Q\rangle$ on a total momentum equal zero ($\vec{P} = 0$) then reads :

$$\hat{P}^{\vec{0}} |Q\rangle = \frac{1}{(2\pi)^3} \int d^3x \, \exp\left\{-\mathrm{i}\hat{\vec{P}} \cdot \vec{x}\right\} |Q\rangle = \frac{1}{(2\pi)^3} \int d^3x \, |Q(\vec{x})\rangle \,, \tag{2.25}$$

where $e^{-\mathrm{i}\hat{\vec{P}}\cdot\vec{x}}$ acts as a translation operator which shifts the many-body wave function by a distance $\vec{x}$.

The matrix elements of an operator $\hat{O}$ with the projected many-body function $|Q_0\rangle$ can be calculated as follows

$$\langle Q_0| \hat{O} |Q_0\rangle = \langle Q| \hat{P}^{\vec{P}\dagger} \hat{O} \hat{P}^{\vec{P}} |Q\rangle = \langle Q| \hat{O} \hat{P}^{\vec{P}} |Q\rangle = \frac{1}{(2\pi)^3} \int d^3x \, \langle Q| \hat{O} |Q(\vec{x})\rangle \,, \tag{2.26}$$

where we expect that the operator $\hat{O}$ commutes with $\hat{\vec{P}}$.

It is straightforward to show that for an operator describing the kinetic energy of the center of mass $\hat{T}_{cm} = \frac{\hat{\vec{P}}^2}{2M}$is such a matrix element equals to zero.

2.5.2 Parity projection

We need to get the many-body state $|Q\rangle$ which is an eigenstate of the parity operator $\hat{\Pi}$ with either odd or even parity eigenvalue π. This is achieved using the parity projection operator

$$\hat{P}^{\pi} = \frac{1}{2}\left(1 + \pi\hat{\Pi}\right). \tag{2.27}$$

The matrix element of an operator $\hat{O}$ with the parity projected many-body state $|Q^{\pi}\rangle$ can be calculated as follows

$$\langle Q^{\pi}| \hat{O} |Q^{\pi}\rangle = \langle Q| \hat{P}^{\pi} \hat{O} \hat{P}^{\pi} |Q\rangle = \langle Q| \hat{O} \hat{P}^{\pi} |Q\rangle = \frac{1}{2}\left(\langle Q| \hat{O} |Q\rangle + \pi \langle Q| \hat{O}\hat{\Pi} |Q\rangle\right), \tag{2.28}$$

where we again assume that the operator $\hat{O}$ and parity operator $\hat{\Pi}$ commute.

2.5.3 Angular momentum projection

The angular momentum projection is performed using the following operator [11]

$$\hat{P}^J_{MK} = \frac{2J+1}{8\pi^2} \int d\Omega {D^J_{MK}}^*(\Omega) \hat{R}(\Omega), \tag{2.29}$$

where $\hat{R}(\Omega)$ denotes the rotation operator (2.9), J total angular momentum, M and K its third projection(doplnit) and (doplnit), respectively, and ${D^J_{MK}}^*(\Omega)$ stands for Wigner D-function

$$D^J_{MM'}(\Omega) = \langle JM | \hat{R}(\Omega) | JM' \rangle . \tag{2.30}$$

Therefore the many-body state $|Q\rangle$ projected on correct parity, angular momentum and zero center of mass momentum can be written as

$$\left| Q; J^\pi MK; \vec{P} = 0 \right\rangle = \hat{P}^J_{MK} \hat{P}^\pi \hat{P}^{\vec{0}} |Q\rangle . \tag{2.31}$$

However the projected states (2.31) are not linear independent. To get orthogonal eigenstates we have to perform "K-mixing" procedure [1].

2.5.4 Variation after projection and projection after variation

The many-body state obtained from the minimization can be projected on the correct center of mass momentum, parity and angular momentum before or after the variation process. The latter possibility can be used only as the first approximation, because we do not minimize the expectation value of Hamiltonian within the correct energy subspace. Therefore, to get better results for deformed nuclei with cluster structure, we should use the first possibility. The variation after projection process is however much more computationally demanding and thus can be performed only for light nuclei [1].

Chapter 3

Interaction

Taking into account only the two-body interaction part $\hat{V}$ of the Hamiltonian operator $\hat{H}$, we can decompose $\hat{V}$ into the sum of individual interaction terms.

In the FMD model it is required to have the interaction part $\hat{V}$ written in the coordinate space as a sum of individual interaction terms $\hat{V}_i$ with radial dependent parts $f_i(r)$ and operator $\hat{O}_i$ where r stands for the relative distance $|\vec{x}_1 - \vec{x}_2|$ between two particles

$$\langle \vec{x}_1, \vec{x}_2 | \hat{V} | \vec{x}_1, \vec{x}_2 \rangle = \hat{V}_1 + \hat{V}_2 + \ldots + \hat{V}_n = f_1(r)\hat{O}_1 + f_2(r)\hat{O}_2 + \ldots + f_n(r)\hat{O}_n. \quad (3.1)$$

In order to be possible to evaluate the matrix elements in (2.21) analytically, the radial dependent parts corresponding to each interaction term in (3.1) are expressed as the sum of Gaussians

$$f(r) \approx \sum_i \gamma_i \exp\left\{ -\frac{(\vec{x}_1 - \vec{x}_2)^2}{2\kappa_i} \right\}, \quad (3.2)$$

where γ_i and κ_i denote the fitting parameters. The procedure allows to evaluate analytically matrix elements of the most relevant interaction terms $\hat{V}_i$.

In the search for the minima of the ground states (2.22), the expectation value of $\hat{H} - \hat{T}_{cm}$ and its gradient with respect to all the parameters in (2.4) have to be calculated in each iteration step. To calculate these expectation values and corresponding gradients in each evaluated step numerically would be in the case of larger number of particles time-demanding and more importantly, the approximate values of the gradient could cause convergence to "false" local minima during the optimization. Therefore the analytical calculation of matrix elements is very important for the optimization process.

3.1 Matrix elements

The matrix element of the interaction term with the radial part $f(r)$ expressed as a sum of Gaussians (3.2) can be written in the following form

$$\begin{aligned}\langle q_k, q_l | \hat{V}_j | q_m, q_n \rangle = \int d^3x_1 d^3x_2 \left\langle a_k, \vec{b}_k; a_l, \vec{b}_l \right| \left. \vec{x}_1; \vec{x}_2 \right\rangle f_j(|\vec{x}_1 - \vec{x}_2|) \\ \langle \chi_k, t_k; \chi_l, t_l | \hat{O}_j | \chi_m, t_m; \chi_n t_n \rangle \left\langle \vec{x}_1; \vec{x}_2 \right| \left. a_m, \vec{b}_m; a_n, \vec{b}_n \right\rangle ,\end{aligned} \tag{3.3}$$

where $\hat{V}_j$ stands for the j-th interaction term and the notation for single particle state parameters is used (2.4).

The most simple central interaction has in the position space only the radial dependent part, thus it can be written as

$$\langle \vec{x}_1, \vec{x}_2 | \hat{V}_c | \vec{x}_1, \vec{x}_2 \rangle = f(r)\hat{1} \approx \sum_i \gamma_i \exp\left\{ -\frac{(\vec{x}_1 - \vec{x}_2)^2}{2\kappa_i} \right\} \hat{1} \tag{3.4}$$

and the matrix elements are of the form

$$\begin{aligned}\langle q_k, q_l | \hat{V}_c | q_m, q_n \rangle \approx \sum_i \gamma_i \int d^3x_1 d^3x_2 \left\langle a_k, \vec{b}_k; a_l, \vec{b}_l \right| \left. \vec{x}_1; \vec{x}_2 \right\rangle \exp\left\{ -\frac{(\vec{x}_1 - \vec{x}_2)^2}{2\kappa_i} \right\} \hat{1} \\ \left\langle \vec{x}_1; \vec{x}_2 \right| \left. a_m, \vec{b}_m a_n, \vec{b}_n \right\rangle S_{km} S_{ln} T_{km} T_{ln} = \sum_i V_{c\ klmn}^{(i)},\end{aligned} \tag{3.5}$$

where the matrices S_{km}, S_{ln}, T_{km} and T_{ln} are defined in (C.1).

It is straightforward to show that for the interaction term $\hat{V}_i$ the matrix elements have to be calculated only once. The analytical expression as a function of the parameters κ_i and γ_i allows to calculate the interaction term with a general radial dependent part $f_i(r)$.

Most matrix elements for particles with the same mass have been evaluated in ref. [4] . We derived analytical expressions for the matrix elements which involve particles with different masses.(not only for protons and neutrons but also for hyperons).

3.2 VolkovV2-M0.0 interaction

In order to test the zero-strangeness part of the FMD program and to compare the calculated results with [4] the effective VolkovV2 interaction with Majorana exchange parameter M0.0 [7] was used. The interaction is suitable for the proper

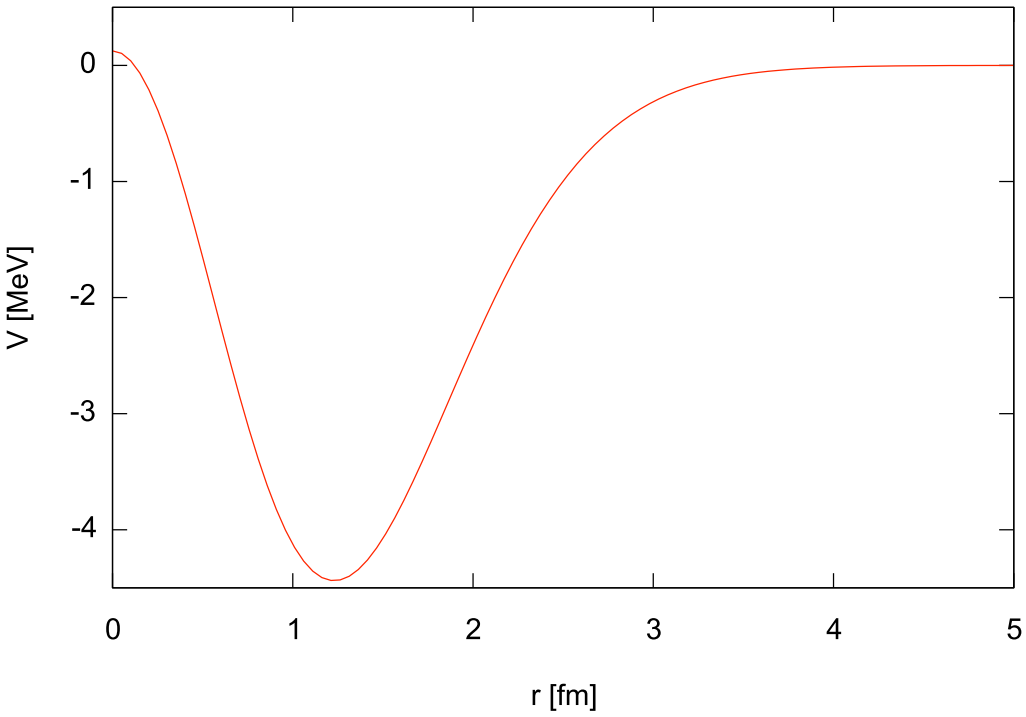

Figure 3.1: The radial dependence of the central part V_c of the VolkovV2-M0.0 interaction expressed as the sum of two Gaussians with parameters given in Tab. 3.1.

description of the s-shell nuclei (^{3}H, ^{4}He). It includes only one central interaction term $\hat{V}_c$ and thus the whole interaction is given by the radial dependent function $f(r)$ as in (3.4). The radial function is expressed by the sum of two Gaussians (3.2). The fitting parameters of the VolkovV2-M0.0 interaction are given in Tab.3.1.

Table 3.1: The values of the parameters γ_i, κ_i for the VolkovV2-M0.0 interaction. [4]

	γ_i [fm^{-1}]	κ_i [fm^2]
V_c	0.077472	0.51005
V_c	-0.076838	1.62000

In Fig.3.1 we present the radial dependent function $f(r)$ expressed as a sum of two Gaussians with the parameters from Tab.3.1.

Chapter 4

FMD program

The main goal of the program is to calculate the ground as well as excited states of light hypernuclei and to study their structure with the FMD model. In the first stage, we decided to focus on the construction and testing of non-strange part of the code calculating ordinary light nuclei. Our results were compared with nuclear data as well as equivalent calculations of GSI.

The nucleon part of the program is used to calculate and to compare the results for zero-strangeness nuclei with the calculation in [4]. The entire zero-strangeness part of the program was successfully checked and the code is now prepared for the further extensions to the strangeness sector.

We chose the object oriented C++ as the programming language to create an object oriented framework which was, from the very beginning, able to treat various baryons with different isospin, strangeness and mass. As mentioned above, the main objective is to extend the program to strange particles $(\Lambda, \Sigma^0, \Sigma^-, \Sigma^+, ..)$. Therefore the existing code is written in the most general form and our extension is straightforward.

The expectation value of the underlaying Hamiltonian was minimized using the quasi-Newton method Software for Large-Scale Bound-constrained Optimization L-BFGS-B [10]. This method and all the related libraries are written in FORTRAN 99 notation. For the linear algebra operations we use the Eigen project libraries [12] written in C++.

All procedures and functions are called from different header files to keep the FMD code clear and easy-to-other improvements. Each header file declares thematically close procedures and functions and is briefly described in Tab.4.1.

The structure of the FMD program is described in Fig. 4.1. There are three parts of the diagram which are solely marked by different colors. The blue is related to the calculations including the trial parameters of the many-body state. The green color denotes the part working with the interactions and the orange color indicates

Table 4.1: The description of the contents of the individual components of the FMD program.

file	content
FMD11.cpp	main body of the program
particle.h	object class to store the single particle state parameters
matrices.h	function and procedures to calculate the auxiliary matrices
interaction.h	functions, procedures and classes using the interaction
observables.h	functions defining matrix elements of the observables
diagnostic.h	diagnostic functions for monitoring the performance of the program
input.txt	parameters of the trial many-body state
interaction.txt	information defining the interactions

the minimization process.

4.1 Input parameters

The architecture of the program allows to read all the input data and parameters from the text files. The file *input.txt* (see Fig. 4.1) defines the trial nuclear many-body state (2.14) which is needed as an input to the minimization process. It provides the information about the parameters (2.4) and isospin of each single particle state (2.1). The parameters defined in this text file are adjusted before the start of the FMD program.

The interaction between nucleons (baryons) is defined in the text file carrying the name of the potential (denoted "*potential.txt*" in Fig. 4.1). The file contains the following information : the number of operator terms (3.1), the type of each interaction term and the parameters of the Gaussians γ_i, κ_i which represent the radial dependence of the interaction term (3.2). The name of the file has to be specified as an argument to the FMD program.

4.2 Minimization procedure

The minimization process is schematically described in the FMD program flow chart in Fig. 4.1. First, the input parameters defining the interaction and the trial many-body function are load and stored.

The auxiliary matrices in Appendix C are calculated and stored using the information about the many-body state. These matrices are a very useful tool for speeding up the minimization process. Mainly from the expression (3.3) one can see

that many analytical calculations just involve integrations over the gauss functions and their solutions contain mostly the same expressions. These expressions in a form of auxiliary matrices are given in (C.1) and (C.2).

The minimization loop is denoted in Fig. 4.1 by the orange color. Before we start optimization, the expectation value of the Hamiltonian (2.21), the array of the parameters defining the many-body state, and the gradient of the expectation value with respect to all parameters are evaluated. These three objects are then passed to the minimization routine.

The routine gives as an output new values for the parameters describing the many-body state. The previous parameters are updated, all the calculations are performed again and passed to an other iteration as long as the convergence of the Hamiltonian expectation value and of gradient is achieved.

4.3 Output data

When the routine successfully converges, the parameters defining the many-body state with the minimum energy are obtained and written. The results of the calculation contain: the binding energy of the system, the parameters defining the particular (hyper)nuclear state and technical information about the minimization process.

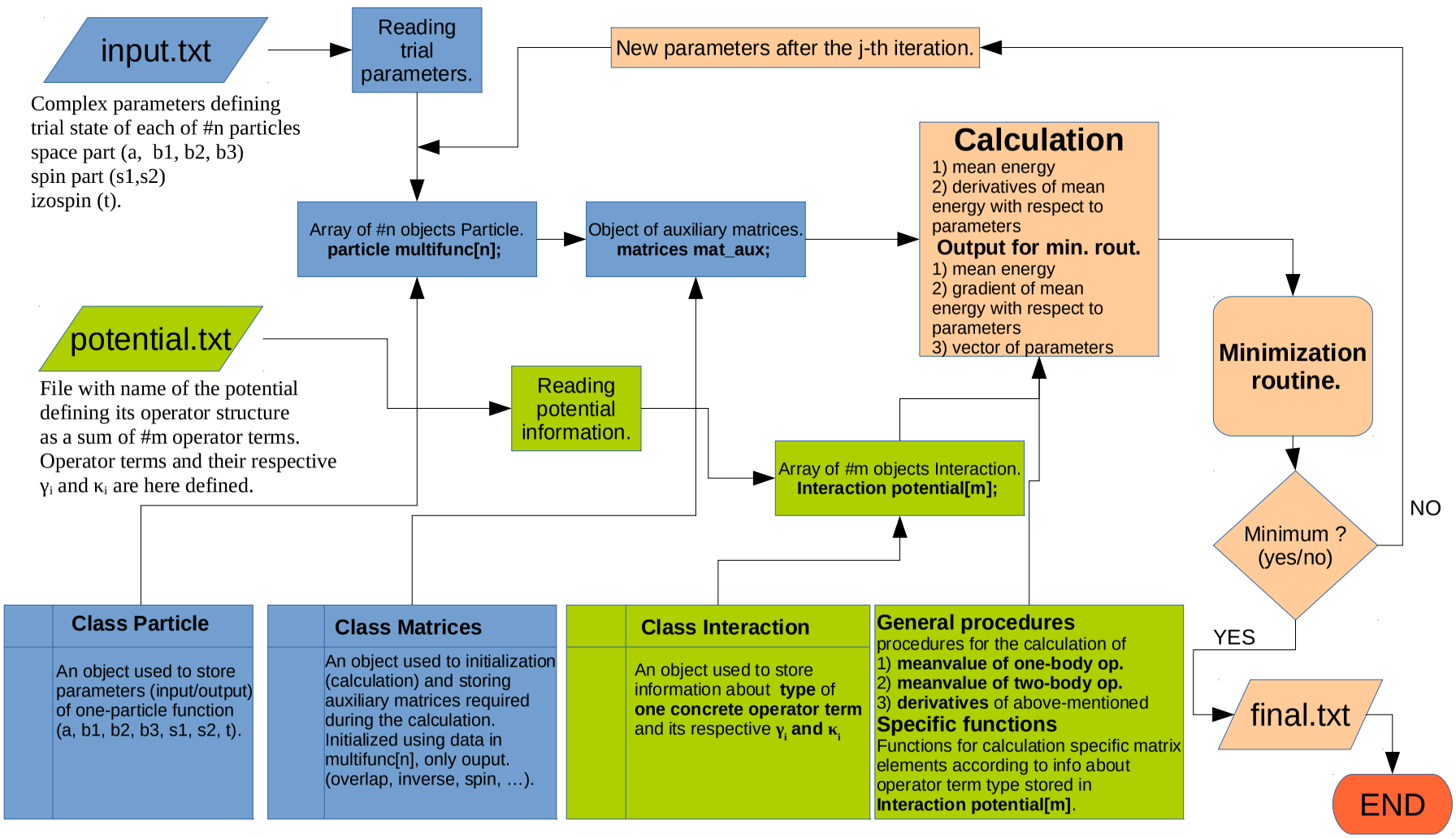

Figure 4.1: The Fermion Molecular Dynamics flow chart describing the structure of the FMD program. The blue part is related to the calculations including the trial parameters of the many-body state only. The green denotes the part working with the interaction and the orange color indicates the minimization process.

Chapter 5

Results

We performed FMD calculations of the s-shell nuclei ^{3}H and ^{4}He. The interaction between nucleons was described using the VolkovV2 effective interaction with the Majorana exchange parameter M0.0 Tab. 3.1. We calculated binding energy, parameters of many-body state and one-body density of the above nuclei.

In order to examine the computational complexity of the program we also minimized the binding energy of the ^{5}He and ^{6}He systems. Since the Volkov interaction does not describe these heavier nuclei properly we do not present the corresponding physical results. We just compare and discuss the duration of the minimization process for ^{3}H, ^{4}He, ^{5}He and ^{6}He.

5.1 Ground state of ^{3}H

In general ,there are no restrictions how to set the initial many-body state of ^{3}H. However, we chose the parameters, so that the trial state fulfills the following conditions: we claim to have each single particle state at rest and the relative distance between the mean positions of single particle states (2.6) is approximately 1 fm. The first condition ensures that none of the particles leaves the system during the minimization process. This is done by setting the expectation value of corresponding single particle state momenta to zero (2.8). The latter condition helps to reduce the number of iterations since the particles are located in the region of strongly attractive force (see Fig. 3.1). The parameters of such trial state are given in Tab. 5.1.

Table 5.1: The initial parameters of the ^{3}H trial state.

N	a	$\vec{b} = (b_1, b_2, b_3)$	$\chi = (\chi^{\uparrow}, \chi^{\downarrow})$	T_3
1	0.5+0.5i	(0.7,0,0)	(0.5+0.5i,0.4+0.4i)	0.5
2	0.6+0.6i	(0,0.7,0)	(0.2+0.2i,0.12+0.12i)	-0.5
3	0.4+0.4i	(0,0,0.7)	(0.3+0.3i,0.65+0.65i)	-0.5

We minimized the expectation value of the total Hamiltonian minus the kinetic energy of the center of mass (2.22) $\hat{H} - \hat{T}_{cm} = \hat{T}_k + \hat{V} - \hat{T}_{cm}$. We reached the minimum for the binding energy $E = -7.19$ MeV. The parameters of the single particle states corresponding to the ground state of ^{3}H are given in Tab. 5.2.

Table 5.2: The resulting values of the single particle states parameters (2.4) relevant to ^{3}H ground state with the binding energy $E = -7.19$ MeV.

1			
Re a	2.49996	Im a	0
Re b_1	0.23333	Im b_1	0.00252
Re b_2	0.23333	Im b_2	0.00251
Re b_3	0.23333	Im b_3	-0.00503
Re $\chi^{\uparrow}$	0.5	Im $\chi^{\uparrow}$	0.5
Re $\chi^{\downarrow}$	0.4	Im $\chi^{\downarrow}$	0.4
T_3	0.5		
2			
Re a	2.49694	Im a	0
Re b_1	0.23333	Im b_1	0.00252
Re b_2	0.23333	Im b_2	0.00251
Re b_3	0.23333	Im b_3	-0.00503
Re $\chi^{\uparrow}$	0.28813	Im $\chi^{\uparrow}$	0.28813
Re $\chi^{\downarrow}$	-0.13656	Im $\chi^{\downarrow}$	-0.13656
T_3	-0.5		
3			
Re a	2.49694	Im a	0
Re b_1	0.23333	Im b_1	0.00252
Re b_2	0.23333	Im b_2	0.00251
Re b_3	0.23333	Im b_3	-0.00503
Re $\chi^{\uparrow}$	0.19853	Im $\chi^{\uparrow}$	0.19853
Re $\chi^{\downarrow}$	0.69090	Im $\chi^{\downarrow}$	0.69090
T_3	-0.5		

The value of the binding energy of ^{3}H is in agreement with the FMD calculations

of T. Neff [4]. The comparison with the other results is in Tab. 5.3.

Table 5.3: The binding energy E_B of ^{3}H calculated by FMD model, by GFMC model and experimental value.

Model	E_B[MeV]
this work (VolkovV2 potential)	-7.19
FMD model (MTV-UCOM potential) [4]	-6.49
GFMC AV18 [13]	-7.61
experimental value [13]	-8.48

In order to calculate the nuclear density of the ^{3}H ground state, the resulting state Tab. 5.2 is shifted, so that the center of mass lies in the center of the coordinate system. In Fig. 5.1 the nuclear density ρ of ^{3}H in the units of the nuclear saturation density $\rho_0 = 0.16$ fm^{-3} is displayed.

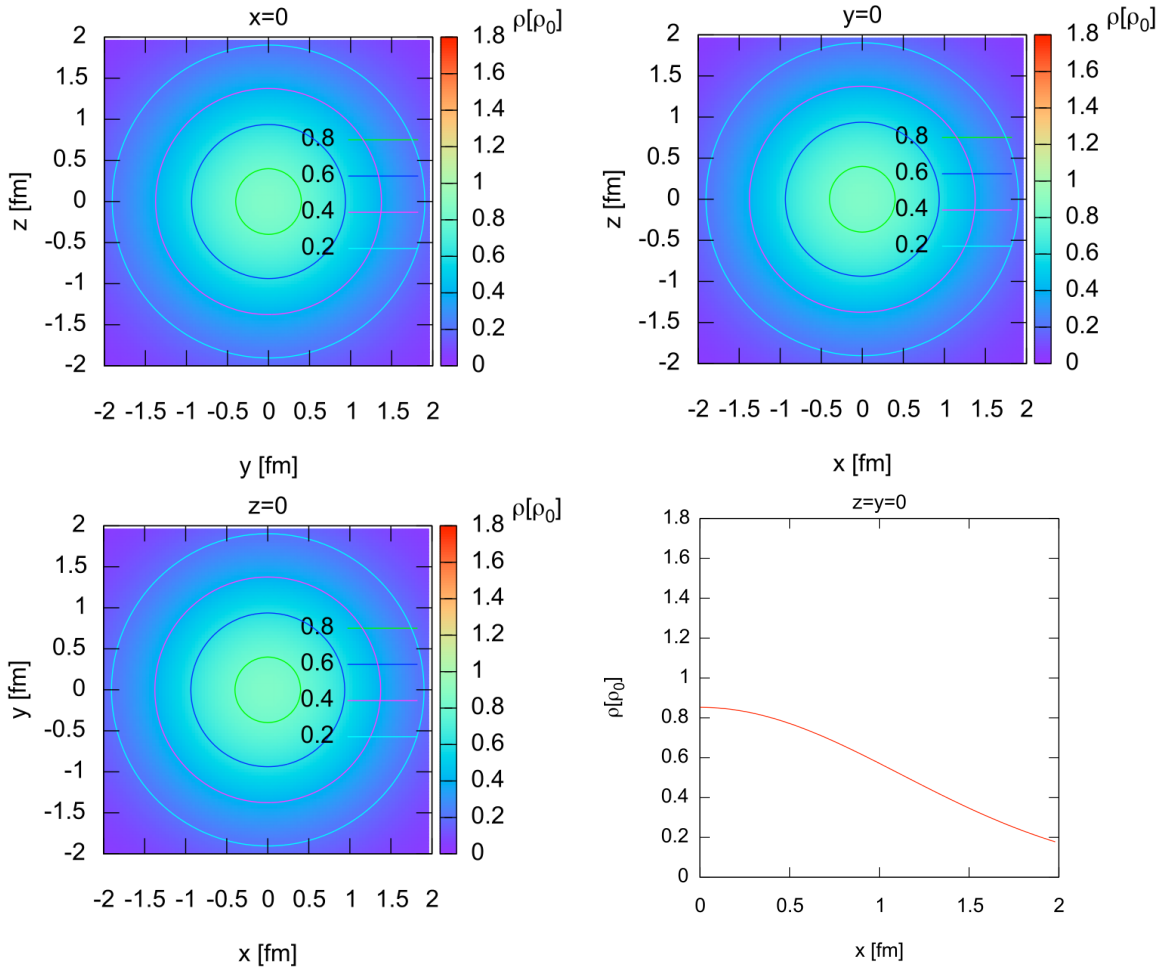

Figure 5.1: The density ρ of the ^{3}H ground state in the units of the nuclear saturation density $\rho_0 = 0.16$ fm^{-3}. The density is successively plotted in x=0, y=0, z=0 plane and y=z=0 cut.

5.2 Ground state of ^{4}He

The FMD calculation of the ground state of ^{4}He is analogous to ^{3}H. The initial parameters of the many-body state are shown in Tab. 5.4. For one proton and two neutrons we set the identical values as in the previous calculation of ^{3}H . The last proton was placed on the x-axis, at a distance of 1 fm from the neutrons and sufficiently close to the remaining proton.

Table 5.4: The initial parameters of the ^{4}He trial state.

N	a	$\vec{b} = (b_1, b_2, b_3)$	$\chi = (\chi^{\uparrow}, \chi^{\downarrow})$	T_3
1	0.5+0.5i	(0.7,0,0)	(0.5+0.5i,0.4+0.4i)	0.5
2	0.6+0.6i	(0,0.7,0)	(0.2+0.2i,0.12+0.12i)	-0.5
3	0.4+0.4i	(0,0,0.7)	(0.3+0.3i,0.65+0.65i)	-0.5
4	0.3+0.3i	(-0.7,0,0)	(0.5+0.5i,0.4+0.4i)	0.5

The binding energy of the ^{4}He ground state was calculated as $E = -28.79$ MeV. The parameters of the corresponding many-body state are presented in Tab. 5.5. The result is satisfactory and consistent with the calculation of T. Neff [4]. The comparison with other theoretical values and experimental results is given in Tab. 5.6.

Table 5.5: The resulting values of the single particle states parameters (2.4) relevant to the ^{4}He ground state with the binding energy $E = -28.79$ MeV.

1				2			
Re a	1.88016	Im a	0	Re a	1.87813	Im a	0
Re b_1	0	Im b_1	0.00941	Re b_1	0	Im b_1	0.00943
Re b_2	0.17499	Im b_2	-0.01085	Re b_2	0.17500	Im b_2	-0.01083
Re b_3	0.17499	Im b_3	0.00165	Re b_3	0.17500	Im b_3	0.00164
Re $\chi^{\uparrow}$	0.53999	Im $\chi^{\uparrow}$	0.55227	Re $\chi^{\uparrow}$	0.25933	Im $\chi^{\uparrow}$	0.25933
Re $\chi^{\downarrow}$	0.31545	Im $\chi^{\downarrow}$	0.33081	Re $\chi^{\downarrow}$	-0.02493	Im $\chi^{\downarrow}$	-0.02493
T_3	0.5			T_3	-0.5		
3				4			
Re a	1.87808	Im a	0	Re a	1.88016	Im a	0
Re b_1	0	Im b_1	0.00943	Re b_1	0	Im b_1	0.00941
Re b_2	0.17500	Im b_2	-0.01083	Re b_2	0.17499	Im b_2	-0.01085
Re b_3	0.17500	Im b_3	0.00164	Re b_3	0.17499	Im b_3	0.00165
Re $\chi^{\uparrow}$	0.25119	Im $\chi^{\uparrow}$	0.25119	Re $\chi^{\uparrow}$	0.44127	Im $\chi^{\uparrow}$	0.42899
Re $\chi^{\downarrow}$	0.67083	Im $\chi^{\downarrow}$	0.67083	Re $\chi^{\downarrow}$	0.45420	Im $\chi^{\downarrow}$	0.46956
T_3	-0.5			T_3	0.5		

Table 5.6: The binding energy E_B of ^{4}He calculated by FMD model, by GFMC model and experimental value.

	E_B[MeV]
this work (VolkovV2 potential)	-28.79
FMD model (ATS3M potential) [4]	-27.89
FMD model (MTV-UCOM potential) [4]	-30.49
GFMC AV18 [13]	-24.07
experimental value [13]	-28.30

In Fig. 5.2 we present the density of the ^{4}He ground state. The relevant many-body wave function is again shifted, so that the center of mass lies in the center of the coordinate system. The density ρ is again calculated in the units of the nuclear saturation density $\rho_0 = 0.16$ fm^{-3}. .

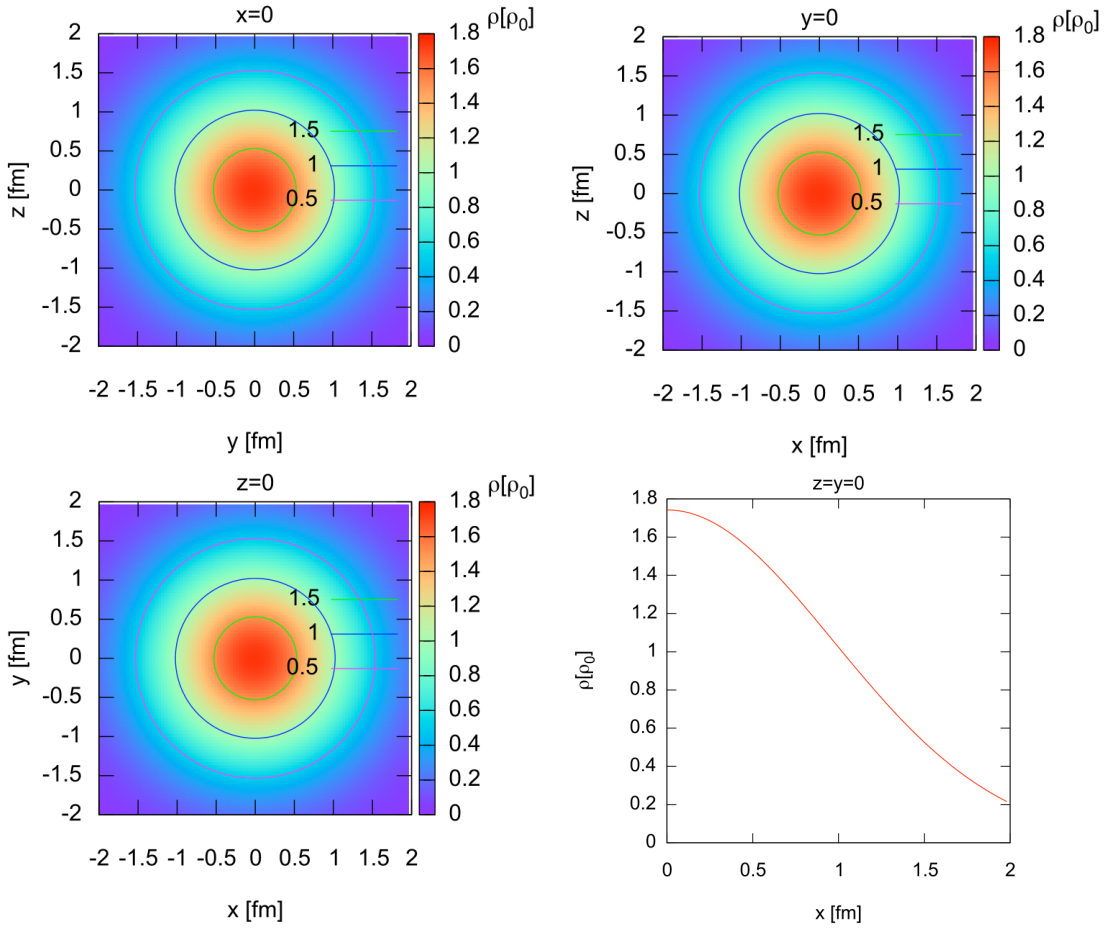

Figure 5.2: The density ρ of the ^{4}He ground state in the units of the nuclear saturation density $\rho_0 = 0.16$ fm^{-3}. The density is successively plotted in x=0, y=0, z=0 plane and y=z=0 cut.

5.3 Computational complexity

We analyzed the time required for the FMD minimization of the ^{3}H, ^{4}He, ^{5}He and ^{6}He systems. The computational complexity significantly grows with the number of particles creating many-body wave function. The minimization process as a function of the mass number A of each aforementioned nucleus is displayed in Fig. 5.3. We observe an exponential dependence on the increasing number of single particle states.

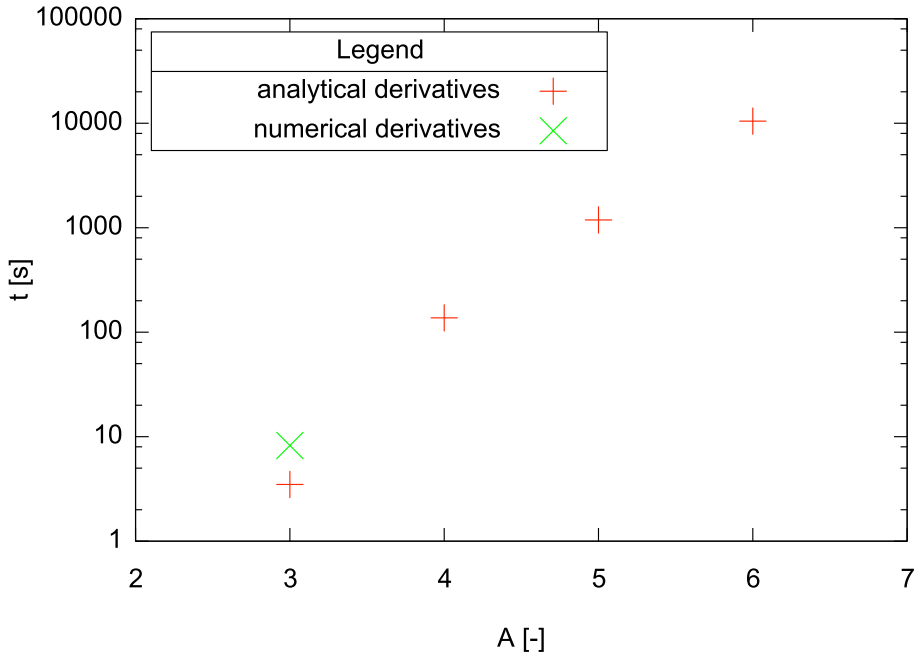

Figure 5.3: The time t required to minimize the expectation value (2.22) of a nucleus with the mass number A. The data are taken from the FMD minimization of ^{3}H, ^{4}He, ^{5}He and ^{6}He using VolkovV2-M0.0 interaction.

We found that the main causes of the above-mentioned computational complexity were the analytical evaluation of the expectation value, gradient and corresponding auxiliary matrices in each iteration. The contribution of the L-BFGS-B minimization algorithm is negligible.

For comparison we performed the calculation of ^{3}H with numerical derivatives (green color in Fig. 5.3). The time of minimization is approximately four times larger. For more complex systems the FMD program didn't converge.

Another feature that affects the time of the minimization process is the complexity of the interaction. The effective VolkovV2-M0.0 interaction Tab. 3.1 is described by one radial dependent term parametrized by the sum of two Gaussians. Consequently, the computational complexity will grow with the number of interaction

terms (3.1) or more precise parametrization of the relevant radial dependent part (3.2).

Chapter 6

Summary

In this research project, we developed the Fermion Molecular Dynamics program for calculating atomic nuclei. Simultaneously, the theoretical foundations of the FMD model were studied in detail with the aim to further extensions of the model to calculations of hypernuclei.

The object oriented FMD code is from the very beginning written in a structured form. We observe that the disadvantage of the FMD model lies in its computational complexity. Therefore, an effective use of computer memory and the order of individual calculations is taken into account. For further extensions of the program, we directly built a universal FMD framework which simply allows to consider particles with arbitrary mass and the third projection of isospin.

The FMD program was tested on the ground states of selected s-shell nuclei. The nucleon-nucleon interaction was described by the VolkovV2 effective potential with Majorana exchange parameter M0.0. The binding energy, parameters of many-body state and nuclear density of the ^{3}H and ^{4}He nuclei were calculated. Our results for the ground states are in agreement with previous FMD calculations [4].

We observe that the computational complexity of the program grows significantly with the number of nucleons. The time duration of the minimization process was studied for ^{3}H, ^{4}He, ^{5}He and ^{6}He. It was found that the computational time increases exponentially with the size of the nuclear system.

In further studies, we are about to include a more sophisticated nucleon-nucleon interaction with spin-orbit, spin-spin and tensor interaction terms. Thus, we will be able to consider larger range of nuclei and examine not only ground states but also excited nuclear states.

However, the main goal of the following research will be the study of hypernuclear structure. Consequently, we will focus on the implementation of the suitable $\Lambda - \mathrm{N}$ interaction. The FMD model requires the two-body potential of the above interaction to be expressed in the operator x-representation. This condition together

with the extension of the FMD program to hypernuclei will be the main task of our further study.

Appendix A

Antisymmetrization of the many-body wave function

The many-body wave function of a nuclear system is antisymmetrized using the operator

$$\hat{A} = \frac{1}{N!} \sum_{P_i} sgn(P_i) \hat{P}_i, \tag{A.1}$$

where N denotes the number of particles and the operator $\hat{P}$ acts as a permutation operator. From the aforementioned definition $\hat{A}$ is a projection operator [1]. Thus, we antisymmetrize the many-body state $|Q\rangle$ as follows

$$|Q_A\rangle = \hat{A} |Q\rangle = \frac{1}{N!} \sum_{P_i} sgn(P_i) \left|q_{P_i(1)}\right\rangle \otimes \ldots \otimes \left|q_{P_i(N)}\right\rangle, \tag{A.2}$$

where q_i denotes the set of parameters specifying the single particle state (2.4).

These parameters also include the isospin of the particle, and thus, within the isospin formalism, the particles are considered indistinguishable and the antisymmetrization is performed regardless of the type of baryon. This is one of the main features of the FMD model

Further, we define the generalized coordinate $|x\rangle$ which determines the position, spin and isospin of a single particle state. In Fermion Molecular Dynamics the antisymmetrized many-body wave function is approximated by the Slater determinant

$$\begin{aligned} \langle x_1, x_2, \ldots, x_N | \, Q_A \rangle &= \frac{1}{N!} \sum_{P_i} sgn(P_i) \left\langle x_1, x_2, \cdots, x_N \right| \, q_{P_i(1)}, q_{P_i(2)}, \ldots, q_{P_i(N)} \rangle \\ &= \frac{1}{N!} \det | \left\langle x_i \right| \, q_j \rangle \, |. \end{aligned} \tag{A.3}$$

The antisymmetrization can be checked by the exchange of two single particle states in (A.3).

The scalar product of an antisymmetrized many-body state can be expressed as follows

$$\begin{aligned}\langle Q_A|\, Q_A\rangle = \langle Q|\, Q_A\rangle &= \frac{1}{N!}\sum_{P_i} sgn(P_i)\left\langle q_1, q_2, \cdots, q_N\right|\, q_{P_i(1)}, q_{P_i(2)}, \ldots, q_{P_i(N)}\big\rangle \\ &= \frac{1}{N!}\sum_{P_i} sgn(P_i)\left\langle q_1\right|\, q_{P_i(1)}\big\rangle \left\langle q_2\right|\, q_{P_i(2)}\big\rangle \cdots \left\langle q_N\right|\, q_{P_i(N)}\big\rangle \\ &= \frac{1}{N!}\mathrm{det}|\,\langle q_i|\, q_j\rangle\,|,\end{aligned} \tag{A.4}$$

where we use the projection feature of antisymmetrization operator.

The definition of antisymmetrization ensures that we antisymmetrize each type of particle separately. This can be shown in the case of two protons p_1, p_2 and one neutron n

$$\begin{aligned}&\langle p_1, p_2, n|\,\hat{A}\,|p_1, p_2, n\rangle = \\ &= \frac{1}{3!}\,\langle p_1, p_2, n|\,\{|p_1, p_2, n\rangle - |p_1, n, p_2\rangle - |p_2, p_1, n\rangle - |n, p_2, p_1\rangle + |p_2, n, p_1\rangle + |n, p_1, p_2\rangle\} = \\ &= \frac{1}{3!}\{\langle p_1|\, p_1\rangle\,\langle p_2|\, p_2\rangle\,\langle n|\, n\rangle - \langle p_1|\, p_1\rangle\,\langle p_2|\, n\rangle\,\langle n|\, p_2\rangle - \langle p_1|\, p_2\rangle\,\langle p_2|\, p_1\rangle\,\langle n|\, n\rangle - \\ &- \langle p_1|\, n\rangle\,\langle p_2|\, p_2\rangle\,\langle n|\, p_1\rangle + \langle p_1|\, p_2\rangle\,\langle p_2|\, n\rangle\,\langle n|\, p_1\rangle + \langle p_1|\, n\rangle\,\langle p_2|\, p_1\rangle\,\langle n|\, p_2\rangle\} = \\ &= \frac{1}{3!}\,\langle p_1|\, p_1\rangle\,\langle p_2|\, p_2\rangle\,\langle n|\, n\rangle - \langle p_1|\, p_2\rangle\,\langle p_2|\, p_1\rangle\,\langle n|\, n\rangle = \\ &= \frac{1}{3!}\,[\langle p_1|\, p_1\rangle\,\langle p_2|\, p_2\rangle - \langle p_1|\, p_2\rangle\,\langle p_2|\, p_1\rangle]\,\langle n|\, n\rangle\,,\end{aligned} \tag{A.5}$$

where we use an orthogonality of $|p\rangle$ and $|n\rangle$ in the isospin space.

It can be easily seen that we are able to antisymmetrize not only states with protons and neutrons but also with other types of particles which differ in the isospin. To extend the FMD model to hypernuclei we antisymmetrize the many-body states including the Λ hyperon with isospin zero.

Appendix B

Derivation of the expectation value formulae

To derive the expectation value formula of the one-body operator $\hat{O}^{[1]}$ we proceed as follows,

$$
\begin{aligned}
&\frac{\langle Q_A|\,\hat{O}^{[1]}\,|Q_A\rangle}{\langle Q_A|\,Q_A\rangle} = \frac{\langle Q|\,\hat{O}^{[1]}\,|Q_A\rangle}{\langle Q|\,Q_A\rangle} = \\
&= \frac{1}{\det|\,\langle q_i|\,q_j\rangle\,|}\{\langle q_1|\otimes\ldots\otimes\langle q_N|\}\sum_k \hat{1}\otimes\ldots\otimes\hat{O}^{[1]}\otimes\ldots\otimes\hat{1} \\
&\{\frac{1}{N!}\sum_{P_m} sgn(P_m)\,\big|q_{P_m(1)}\big\rangle\otimes\ldots\otimes\big|q_{P_m(N)}\big\rangle\} = \\
&= \frac{1}{\det|\,\langle q_i|\,q_j\rangle\,|}\sum_k\sum_{P_m} sgn(P_m)\,\big\langle q_1\big|\,q_{P_m(1)}\big\rangle\ldots\langle q_k|\,\hat{O}^{[1]}\,\big|q_{P_m(k)}\big\rangle\ldots\big\langle q_N\big|\,q_{P_m(N)}\big\rangle = \\
&= \frac{1}{\det|\,\langle q_i|\,q_j\rangle\,|}\sum_k\sum_{P_m} \langle q_k|\,\hat{O}^{[1]}\,\big|q_{P_m(k)}\big\rangle\, sgn(P_m)\,\big\langle q_1\big|\,q_{P_m(1)}\big\rangle\ldots \\
&\ldots\big\langle q_{k-1}\big|\,q_{P_m(k-1)}\big\rangle\,\big\langle q_{k+1}\big|\,q_{P_m(k+1)}\big\rangle\ldots\big\langle q_N\big|\,q_{P_m(N)}\big\rangle = \\
&= \frac{1}{\det|\,\langle q_i|\,q_j\rangle\,|}\sum_{kl}\langle q_k|\,\hat{O}^{[1]}\,|q_l\rangle\,(-)^{k+l}\sum_{P_m} sgn(P_m)\,\big\langle q_1\big|\,q_{P_m(1)}\big\rangle\ldots \\
&\ldots\big\langle q_{k-1}\big|\,q_{P_m(k-1)}\big\rangle\,\big\langle q_{k+1}\big|\,q_{P_m(k+1)}\big\rangle\ldots\big\langle q_n\big|\,q_{P_m(N)}\big\rangle = \\
&= \sum_{kl}\langle q_k|\,\hat{O}^{[1]}\,|q_l\rangle\,\frac{(-)^{k+l}\det|\mathrm{n_{k,l}}|}{\det|\,\langle q_i|\,q_j\rangle\,|} = \sum_{kl}\langle q_k|\,\hat{O}^{[1]}\,|q_l\rangle\,o_{lk},
\end{aligned}
\tag{B.1}
$$

where we consider the non-orthogonality of single particle states. In the last step we use the expression for the element of inverse matrix

$$
o_{lk} = (-)^{k+l}\frac{\det|\mathrm{n_{k,l}}|}{\det|\,\langle q_i|\,q_j\rangle\,|},\ o = n^{-1}, \tag{B.2}
$$

where n is the single particle state overlap matrix (2.16) and $n_{k,l}$ is the single particle state overlap matrix with missing k-th row and l-th column.

The derivation of the expectation value formula of the two-body operator $\hat{O}^{[2]}$ proceeds in a similar but more tedious way. For more information we refer to [1] and [4].

Appendix C

Auxiliary matrices

The calculation time of the FMD program can be considerably diminished by using auxiliary matrices. The elements of such matrices are functions of the many-body state parameters (2.4) and are computed at each iteration step. Thus, the analytical expressions of matrix elements are mostly presented and subsequently programmed as a function of these auxiliary matrices. The notation is adapted from the previous FMD calculations [4]

$$
\begin{aligned}
\lambda_{kl} &= \frac{1}{a_k^* + a_l}, \\
\alpha_{kl} &= \frac{a_k^* a_l}{a_k^* + a_l} = \lambda_{kl} a_k^* a_l, \\
\vec{\pi}_{kl} &= \mathrm{i}\frac{\vec{b}_k^* - \vec{b}_l}{a_k^* + a_l} = \mathrm{i}\lambda_{kl}(\vec{b}_k^* - \vec{b}_l), \\
\vec{\rho}_{kl} &= \frac{a_l \vec{b}_k^* + a_k^* \vec{b}_l}{a_k^* + a_l} = \lambda_{kl}(a_l \vec{b}_k^* + a_k^* \vec{b}_l), \\
R_{kl} &= \left\langle a_k, \vec{b}_k \right| \left. a_l, \vec{b}_l \right\rangle = (2\pi\alpha_{kl})^{3/2} \exp\left(\frac{\vec{\pi}_{kl}^2}{2\lambda_{kl}}\right), \\
S_{kl} &= \left\langle \chi_k^{\uparrow}, \chi_k^{\downarrow} \right| \left. \chi_l^{\uparrow}, \chi_l^{\downarrow} \right\rangle = \chi_k^{\uparrow *} \chi_l^{\uparrow} + \chi_k^{\downarrow *} \chi_l^{\downarrow}, \\
T_{kl} &= \langle t_k | \, t_l \rangle = \delta_{kl}, \\
n_{kl} &= R_{kl} S_{kl} T_{kl}, \\
o_{kl}, &\quad o = n^{-1}.
\end{aligned}
\tag{C.1}
$$

Where λ_{kl}, α_{kl}, $\vec{\pi}_{kl}$ and $\vec{\rho}_{kl}$ denote the auxiliary matrices and R_{kl}, S_{kl}, T_{kl} are overlaps in the respective subspaces. The matrix n_{kl} denotes the single particle state overlap (2.16) and o_{kl} is the element of the inverse overlap matrix.

The computation of two-body matrix elements is facilitated using auxiliary tensors

$$
\begin{aligned}
\alpha_{klmn} &= \alpha_{km} - \alpha_{ln}, \\
\beta_{klmn} &= \mathrm{i}[(a_k^* - a_m)\lambda_{km} + (a_l^* - a_n)\lambda_{ln}], \\
\lambda_{klmn} &= \lambda_{km} + \lambda_{ln}, \\
\theta_{klmn} &= (a_k^*\lambda_{km} + a_l^*\lambda_{ln})(a_m\lambda_{km} + a_n\lambda_{ln}), \\
\vec{\rho}_{klmn} &= \vec{\rho}_{km} - \vec{\rho}_{ln}, \\
\vec{\pi}_{klmn} &= \frac{1}{2}(\vec{\pi}_{km} - \vec{\pi}_{ln}).
\end{aligned}
\tag{C.2}
$$

Appendix D

Derivatives

The derivatives of the expectation value of the Hamiltonian E with respect to the parameters (2.4) have to be calculated analytically. First, recall that each parameter is complex and therefore we must calculate the aforementioned derivatives with respect to its real and imaginary parts. We denote as $p = \mathrm{Re}p + \mathrm{i}\mathrm{Im}p$ some arbitrary parameter from (2.4). Thus, the expectation value of Hamiltonian depends on p and its complex conjugate p^* $E = E(p, p^*)$. Where p^* comes from the bra vector and p comes from the ket vector of the respective single particle state (2.1) in (2.22).

The derivatives of E with respect to Rep and Imp hold the following relations:

$$\begin{aligned}
\frac{\partial E}{\partial \mathrm{Re}\ p} &= \frac{\partial E}{\partial p}\frac{\partial p}{\partial \mathrm{Re}\ p} + \frac{\partial E}{\partial p^*}\frac{\partial p^*}{\partial \mathrm{Re}\ p} = \frac{\partial E}{\partial p} + \frac{\partial E}{\partial p^*} = \left(\frac{\partial E}{\partial p^*}\right)^* + \frac{\partial E}{\partial p^*} = \\
&= \mathrm{Re}\frac{\partial E}{\partial p^*} - \mathrm{i}\mathrm{Im}\frac{\partial E}{\partial p^*} + \mathrm{Re}\frac{\partial E}{\partial p^*} + \mathrm{i}\mathrm{Im}\frac{\partial E}{\partial p^*} = 2\mathrm{Re}\frac{\partial E}{\partial p^*}, \\
\frac{\partial E}{\partial \mathrm{Im}\ p} &= \frac{\partial E}{\partial p}\frac{\partial p}{\partial \mathrm{Im}\ p} + \frac{\partial E}{\partial p^*}\frac{\partial p^*}{\partial \mathrm{Im}\ p} = \mathrm{i}\frac{\partial E}{\partial p} - \mathrm{i}\frac{\partial E}{\partial p^*} = \mathrm{i}\left(\frac{\partial E}{\partial p^*}\right)^* - \mathrm{i}\frac{\partial E}{\partial p^*} = \\
&= \mathrm{i}\mathrm{Re}\frac{\partial E}{\partial p^*} + \mathrm{Im}\frac{\partial E}{\partial p^*} - \mathrm{i}\mathrm{Re}\frac{\partial E}{\partial p^*} + \mathrm{Im}\frac{\partial E}{\partial p^*} = 2\mathrm{Im}\frac{\partial E}{\partial p^*},
\end{aligned} \tag{D.1}$$

where we consider that the expectation value of Hamiltonian E is a real function

$$\frac{\partial E}{\partial p} = \left(\frac{\partial E}{\partial p^*}\right)^*. \tag{D.2}$$

Thus we obtained the following result

$$2\frac{\partial E}{\partial p^*} = \frac{\partial E}{\partial \mathrm{Re}\ p} + \mathrm{i}\frac{\partial E}{\partial \mathrm{Im}\ p}. \tag{D.3}$$

For the derivative of E with respect to p^* we only present the relevant expressions

for one-body $E^{[1]}$ and two-body $E^{[2]}$ parts

$$\frac{\partial E^{[1]}}{\partial p^*} = \sum_l \left[\frac{\partial}{\partial p^*} \langle q_m | \hat{H}^{[1]} | q_l \rangle - \sum_{rs} \left(\frac{\partial}{\partial p^*} \langle q_m | q_r \rangle , \right) o_{rs} \langle q_s | \hat{H}^{[1]} | q_l \rangle \right] o_{lm} \tag{D.4}$$

$$\frac{\partial E^{[2]}}{\partial p^*} = \sum_{kln} \left[\frac{\partial}{\partial p^*} \langle q_m, q_n | \hat{H}^{[2]} | q_k, q_l \rangle - \sum_{rs} \left(\frac{\partial}{\partial p^*} \langle q_m | q_r \rangle \right) o_{rs} \langle q_s, q_n | \hat{H}^{[2]} | q_k, q_l \rangle \right] (o_{km} o_{ln} - o_{lm} o_{kn}), \tag{D.5}$$

where we assume that p is a parameter of the m-th single particle state $|q_m\rangle$. For a precise derivation see [4].

Bibliography

[1] T. Neff, H. Feldmeier, Nucl. Phys. **A 738** (2004) 357.

[2] M. Chernyk, H. Feldmeier, T. Neff, P. von Neumann-Cosel and A. Richter, Phys. Rev. Lett. **98** (2007) 032501.

[3] T. Neff, H. Feldmeier and R. Roth, Prog. in Part and Nucl. Phys **65** (2010) 50.

[4] T. Neff, *Fermionische Molekulardynamik mit Konfigurationsmischungen und realistichen Wechselwirkungen*. Master thesis, TU Darmstadt, 1998.

[5] H. Feldmeier, K. Bieler and J. Schnack, Nucl. Phys. **A 586, 3** (1995) 493.

[6] T. Neff, *Short-Ranged Central and Tensor Correlations in Nuclear Many-Body Systems*. Ph.D. thesis , TU Darmstadt, 2002.

[7] A. Volkov, Nucl. Phys. **74** (1965) 33.

[8] Y Kanada-En'yo, M Kimura, H Horiuchi,*Comptes rendus Physique*, Elsevier, 2003.

[9] H. Horiuchi, Y. Kanada-Enyo and A. Ono, Z. Phys. **A 349** (1994), 279.

[10] R. H. Byrd, P. Lu and J. Nocedal, SIAM Jour. on Sc. and Stat. Comp. **16,5** (1995) 1190.

[11] P. Ring, P. Schuck, *The Nuclear Many-Body Problem* , Springer, 2000.

[12] The Eigen project [online]
URL:<http://eigen.tuxfamily.org>[cit. 12.9.2014]

[13] S. C. Pieper, V. R. Pandharipande, R. B. Wiringa and J. Carlson, Phys. Rev. **C 64** (2001) 014001.